Supporting Information

Co_3O_4/Nitrogen-Doped Graphitic Carbon/Fe_3O_4 Nanocomposites as Reusable Catalysts for Hydrogenation of Quinoline, Cinnamaldehyde, and Nitroarenes

M. Nasiruzzaman Shaikh[1], Mahmoud M. Abdelnaby[2], Abbas S. Hakeem[1], Galal A. Nasser[1] and Zain H. Yamani[1]*

[1]Center of Research Excellence in Nanotechnology (CENT), King Fahd University of Petroleum & Minerals (KFUPM), Dhahran 31261, Saudi Arabia

[2]King Abdulaziz City for Science and Technology – Technology Innovation Center on Carbon Capture and Sequestration (KACST-TIC on CCS), KFUPM, Dhahran, 31261, Saudi Arabia

Corresponding Author

M. Nasiruzzaman Shaikh, *email: mnshaikh@kfupm.edu.sa*

Table of Contents

Catalyst Characterization Techniques	S3-S5
Effect of solvents and pressure on the conversion and selectivity of quinoline hydrogenation at 40 bar H_2 pressure	S6
Raman spectra for the re-used Co_3O_4/N-Gr/Fe_3O_4-800-1and its Raman shifts.	S6
XRD of ZIF-67	S7
FTIR data of prepared catalyst and fresh Fe_3O_4.	S7
ICP-OES data for Co_3O_4/N-Gr/Fe_3O_4-700-0.4, Co_3O_4/N-Gr/Fe_3O_4-800-1 and Co_3O_4/N-Gr/Fe_3O_4-800-1.3 catalysts	S8
EDX of Co_3O_4/N-Gr/Fe_3O_4-800-1	S8
XPS survey of the Co_3O_4/N-Gr/Fe_3O_4-800-1catalyst	S9
Possible reaction pathways for hydrogenation of cinnamaldehyde	S9
Reusability of the catalyst	S10
^1H and ^{13}C NMR spectra	S11-S14
GC-MS Spectra	S15-S16

Catalyst Characterization Techniques

X-ray Diffraction (XRD). X-ray diffraction patterns were recorded on a Rigaku model Ultima-IV diffractometer employing Cu-Kα radiation (λ = 1.5406 Å) at 40 kV and 25 mA over a 2θ range between 20 and 80°.

Surface Area. The total accessible area (S_{BET}) was determined by N_2 physiosorption using ASAP 2020 (Micromeritics, USA).

Transmission Electron Microscopy (TEM). TEM images were acquired at the Instituto de Nanociencia de Aragón (LMA-INA), University of Zaragoza, Spain, on a TEM (Titan, FEI) operated at 200 kV with 4k × 4k CCD camera (Ultra Scan 400SP, Gatan). High resolution transmission electron microscopic (HRTEM) images were obtained in an image corrected Titan (FEI) at a working voltage of 300 KV. X-ray Energy Dispersive Spectra (EDS) were obtained with an EDAX detector The TEM samples were prepared by dropping on a copper grid from an ethanolic suspension and drying at room temperature.

Scanning Transmission Electron Microscopy-High Angle Annular Dark Field (STEM-HAADF). STEM-HAADF images were obtained using a Cs-probe-corrected Titan (ThermoFisher Scientific, formerly FEI) at a working voltage of 300 KV, coupled with an HAADF detector (Fischione).

Scanning Electron Microscope (SEM). Samples for SEM were prepared from ethanolic suspensions on single-sided alumina tape placed on alumina stubs. For the elemental analysis and mapping, the energy-dispersive X-ray spectra (EDS) were collected on a Lyra 3 (Tescan from the Chezch Republic) attachment to the SEM.

Vibrating Sample Magnetometer (VSM). Magnetic susceptibilities were determined at room temperature using a vibrating sample magnetometer (VSM, model PMC Micromag 3900) equipped with a 1 tesla magnet.

Autoclave. Catalytic reactions were performed using Teflon-lined vessels in an autoclave from HiTech, USA (model M010SSG0010-E129A-00022-1D1101), fitted with a pressure gauge and a mechanical stirrer.

Gas Chromatography-Mass Spectrometry (GC-MS). Catalytic products were identified using a Shimadzu 2010 Plus (Japan) gas chromatograph coupled with a mass spectrometer. Disappearance of the reactants and sequential appearance of the products was recorded in real-time, identifying the species in terms of their molecular ion (M^+) by comparing and matching them with the available Wiley library of the mass spectral database, in addition to the identification of mass fragmentation.

Inductively Coupled Plasma Optical Emission Spectrometry (ICP-OES). The amounts of Fe and Co content in the catalyst were determined using inductively coupled plasma optical emission spectrometry (ICP-OES; PlasmaQuant PO 9000 - Analytik Jena**)**. The samples

were first digested in a mixture of dilute HNO_3 and dilute HCl. Calibration curves were prepared for Fe and Co using standard solutions (ICP Element Standard solutions, Merk).

X-ray Photoelectron Spectroscopy (XPS). The surface chemistry was determined using an *X-ray* photoelectron spectroscope (XPS) equipped with an Al-Kα micro-focusing *X-ray* monochromator (ESCALAB 250Xi XPS Microprobe, Thermo Scientific, MA, USA). The chamber pressure was 2×10^{-9} torr. Each XPS spectrum was corrected for steady-state charging by aligning C1s to 284.60 eV. Typical XPS survey spectra of the fabricated films and O1s, $Co2p_{3/2}$, and N1s core-level spectra for the nanocatalyst.

Raman Spectroscopy. The Raman spectra were recorded using a Thermo Scientific DXR Raman spectroscope using DXR 455 nm filter.

Nuclear Magnetic Resonance Spectroscopy. The ^{1}H and ^{13}C solution NMR experiments were performed on a Bruker Advance 400 Spectrometer. ^{1}H and ^{13}C NMR chemical shifts were given as δ values with reference to tetramethylsilane (TMS) as an internal standard.

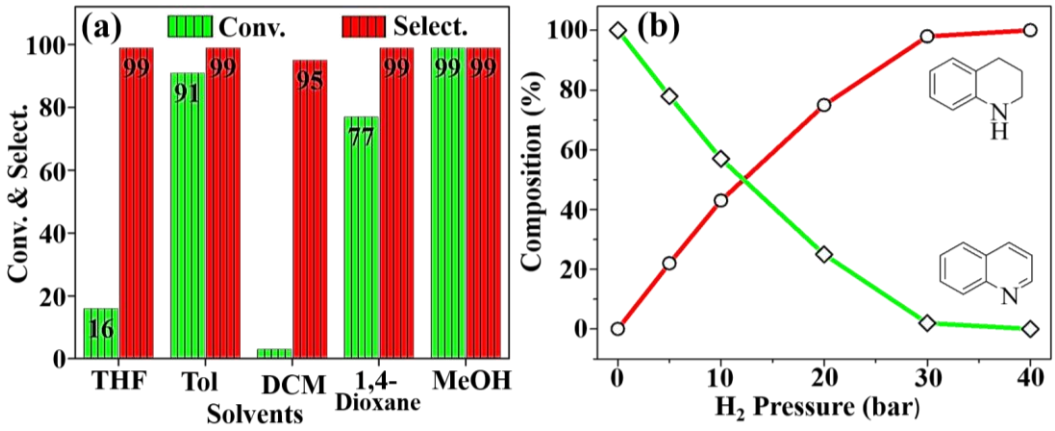

Figure S1. Effect of (a) solvents on the conversion and selectivity of quinoline hydrogenation at 40 bar H_2 pressure; (b) pressure on the formation of py-THQ at 120 °C in 15 h using Co_3O_4/N-Gr/Fe_3O_4-800-1 as the catalyst in methanol.

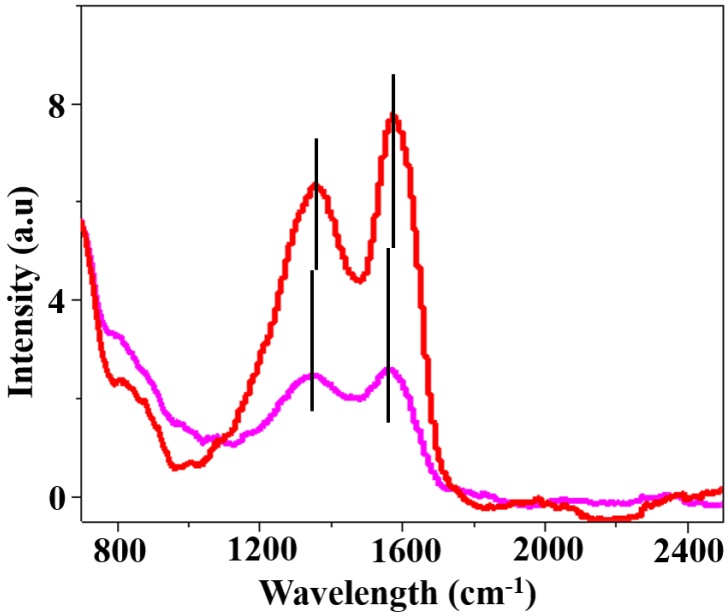

Figure S2. Raman spectra for the re-used Co_3O_4/N-Gr/Fe_3O_4-800-1 and its Raman shifts.

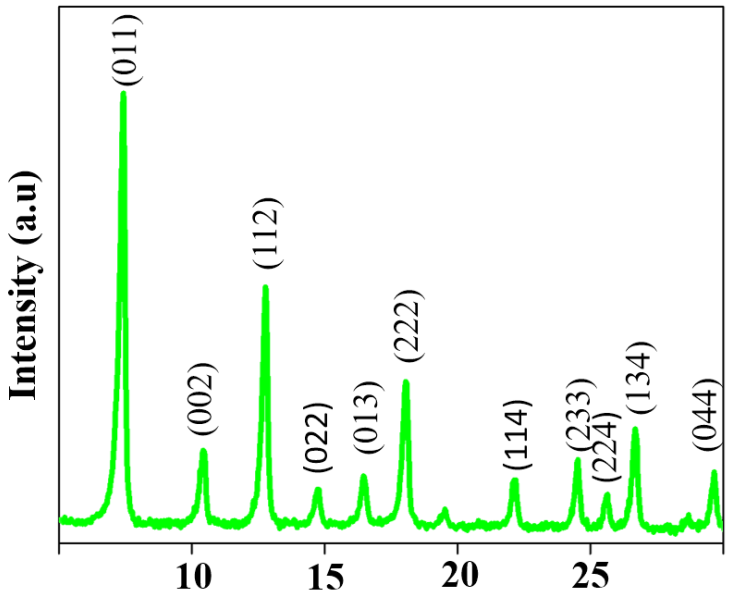

Figure S3. XRD of ZIF-67.

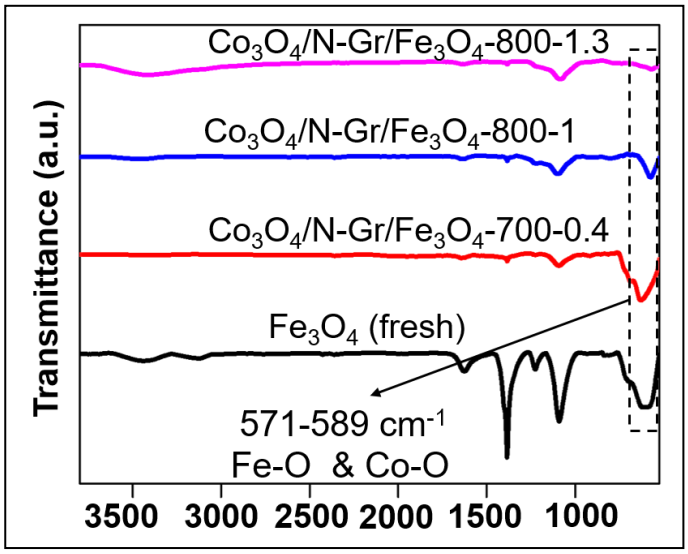

Figure S4. FTIR data of prepared catalysts and fresh Fe_3O_4.

Table S1. ICP-OES data for Co_3O_4/N-Gr/Fe_3O_4-700-0.4, Co_3O_4/N-Gr/Fe_3O_4-800-1 and Co_3O_4/N-Gr/Fe_3O_4-800-1.3 catalysts

Catalyst	Iron	Cobalt	%Cobalt
Co_3O_4/N-Gr/Fe_3O_4-700-0.4	3737	388.2	9.41
Co_3O_4/N-Gr/Fe_3O_4-800-1	3585	924.7	20.49
Co_3O_4/N-Gr/Fe_3O_4-800-1.3	1930	794.7	29.20

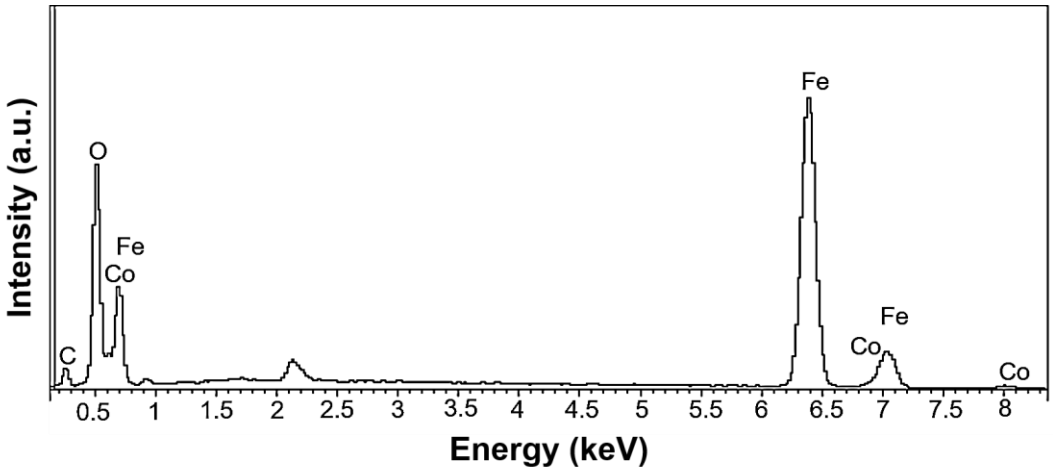

Figure S5. SEM-EDX of Co_3O_4/N-Gr/Fe_3O_4-800-1.

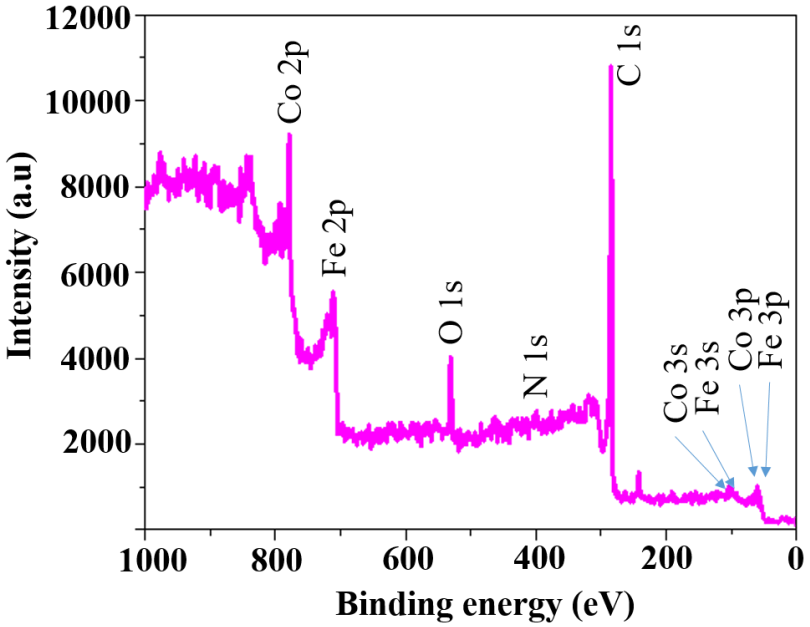

Figure S6. XPS survey of the Co_3O_4/N-Gr/Fe_3O_4-800-1 nanocomposite as catalyst.

Scheme S1. Possible reaction pathways for hydrogenation of cinnamaldehyde

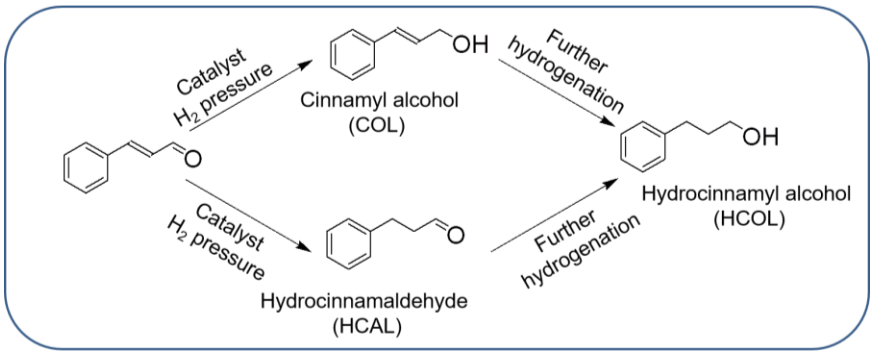

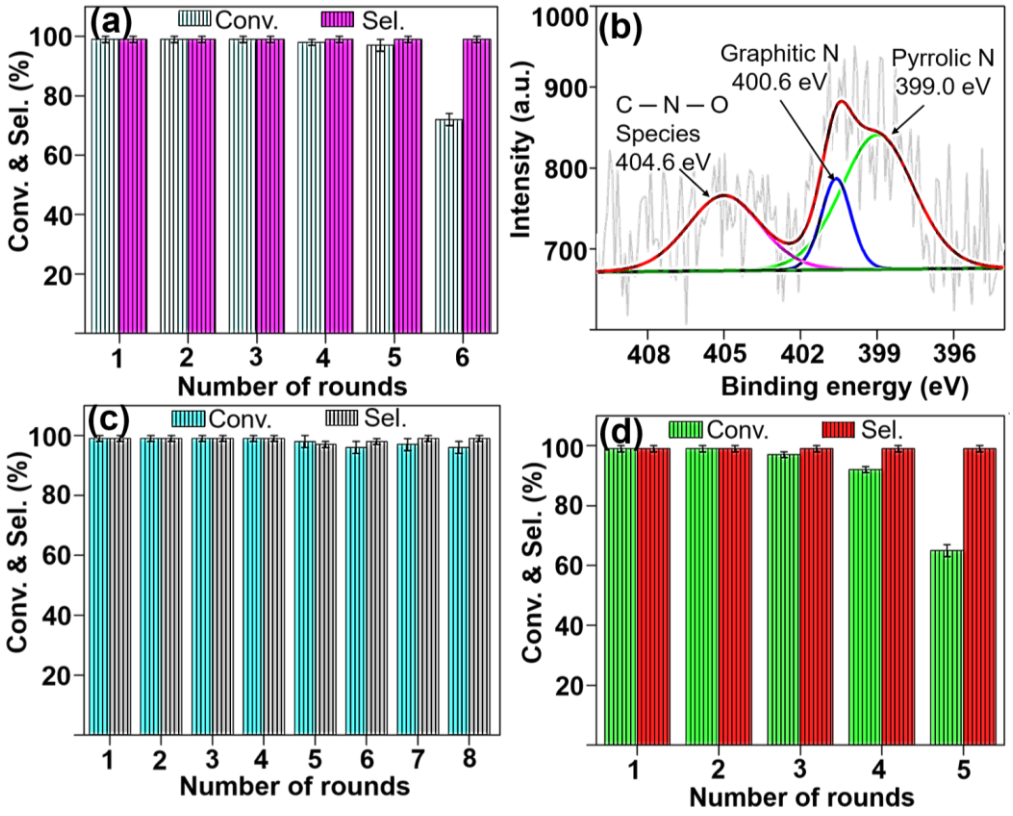

Figure S7. Reusability of the catalyst, Co_3O_4/N-Gr/Fe_3O_4-800-1 nanocomposite, for the hydrogenation of (a) quinolone (b) N1s XPS of the reused catalyst (c) cinnamaldehyde and (d) nitrobenzene.

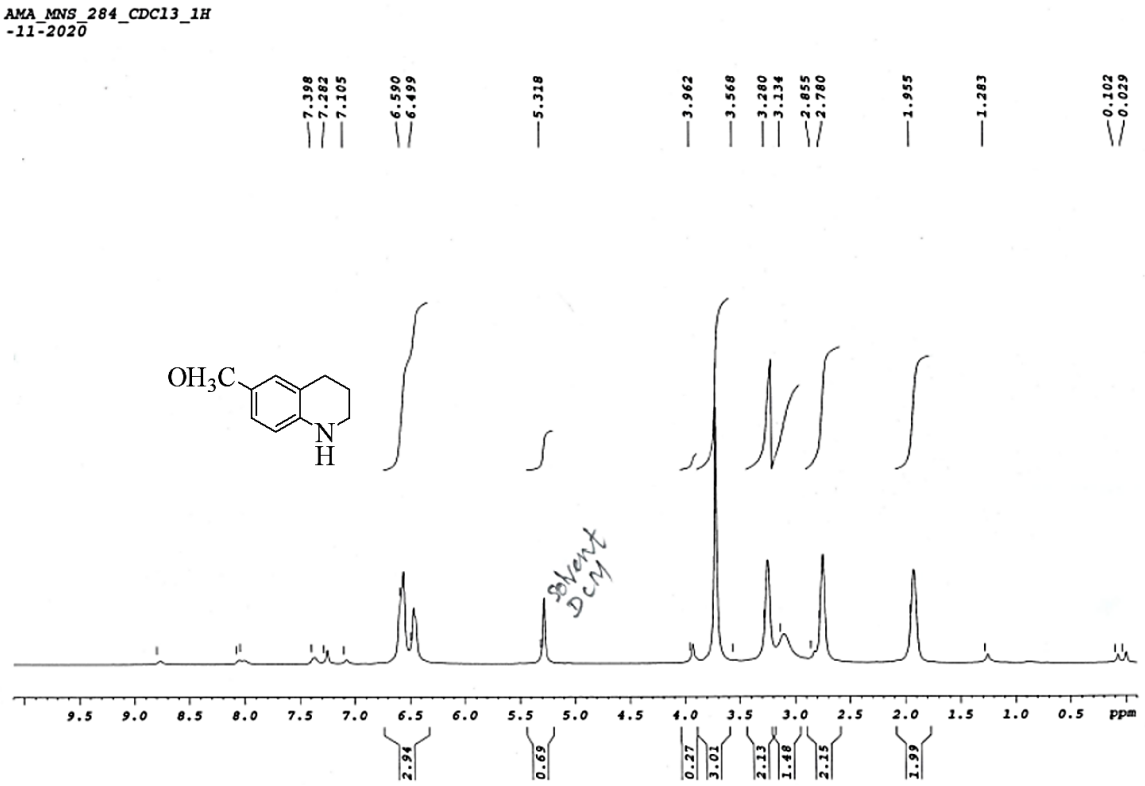

Figure S8. ^{1}H NMR of 6-methoxy-1,2,3,4-tetrahydroquinoline in $CDCl_3$ as solvent.

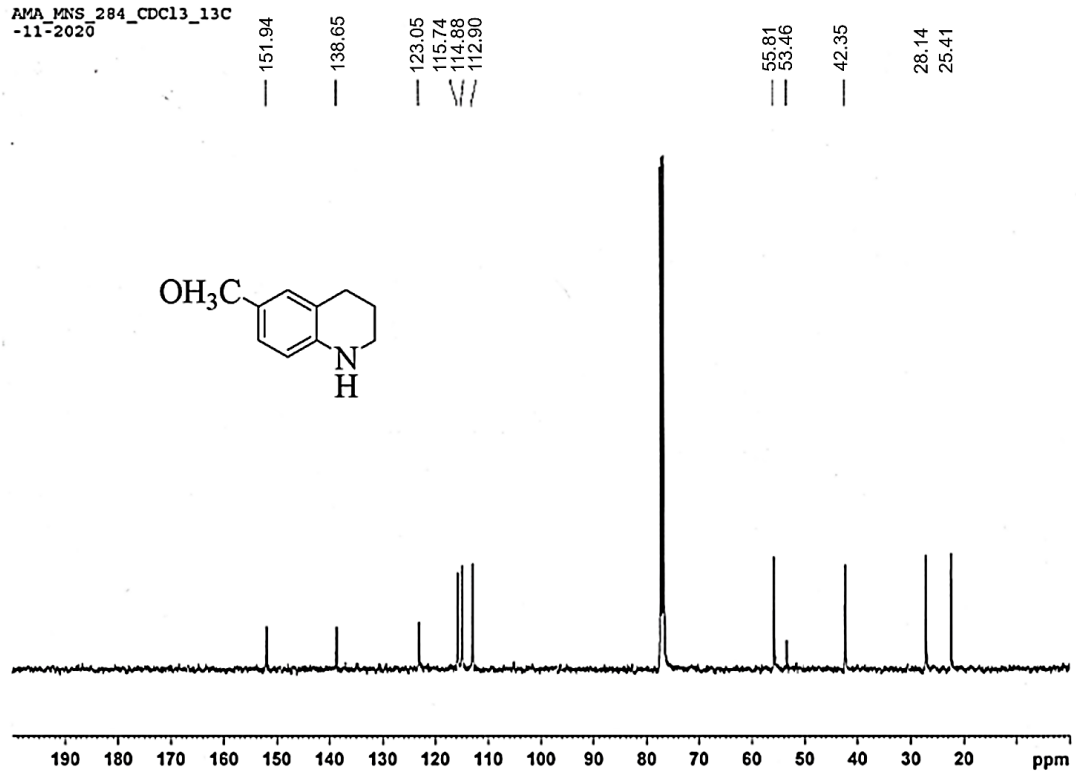

Figure S9. ^{13}C NMR of 6-methoxy-1,2,3,4-tetrahydroquinoline in $CDCl_3$ as solvent.

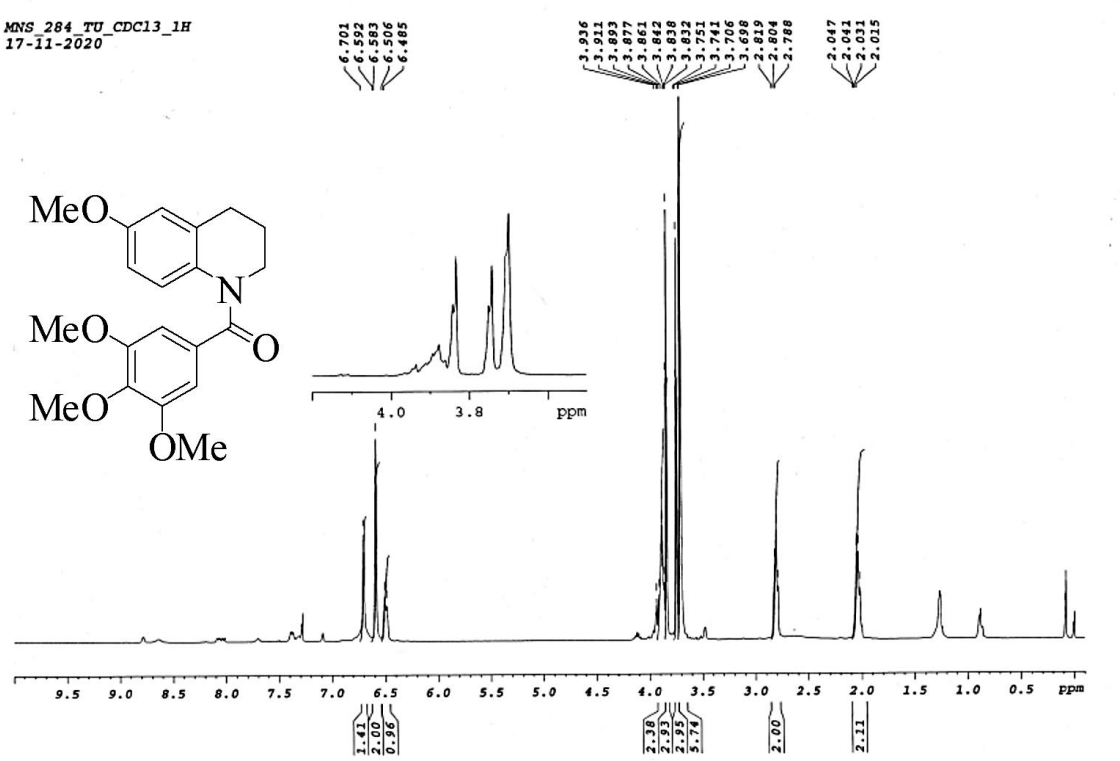

Figure S10. ^{1}H NMR of tubulin polymerization inhibitor in $CDCl_3$ as solvent.

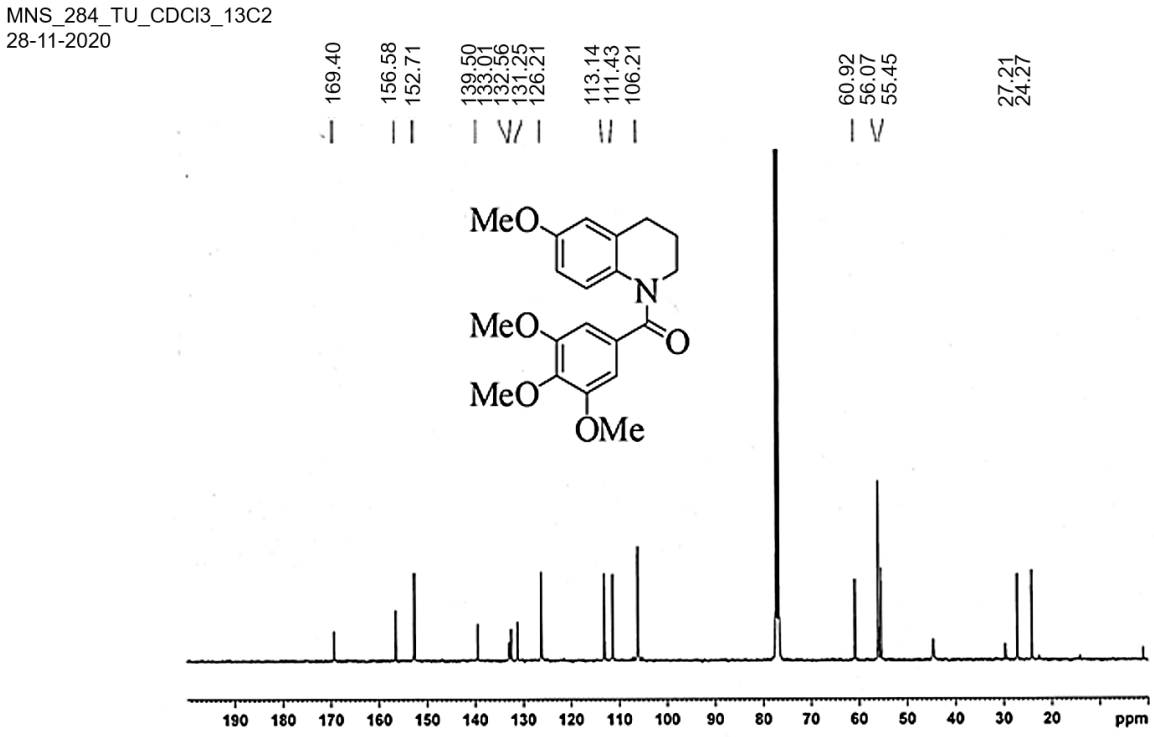

Figure S11. ^{13}C NMR of tubulin polymerization inhibitor in $CDCl_3$ as solvent.

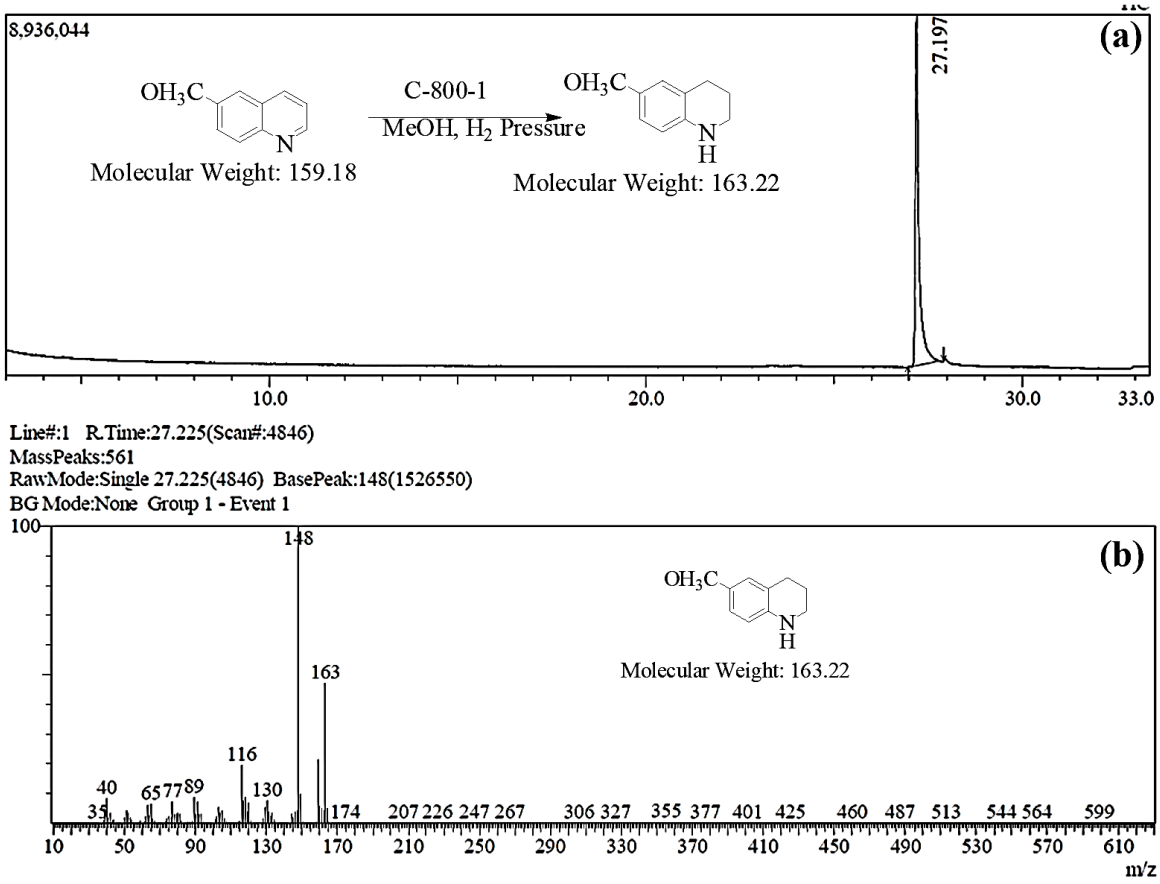

Figure S12. Hydrogenation of 6-methoxy-1,2,3,4-quinoline in methanol (a) GC and (b) MS spectra.

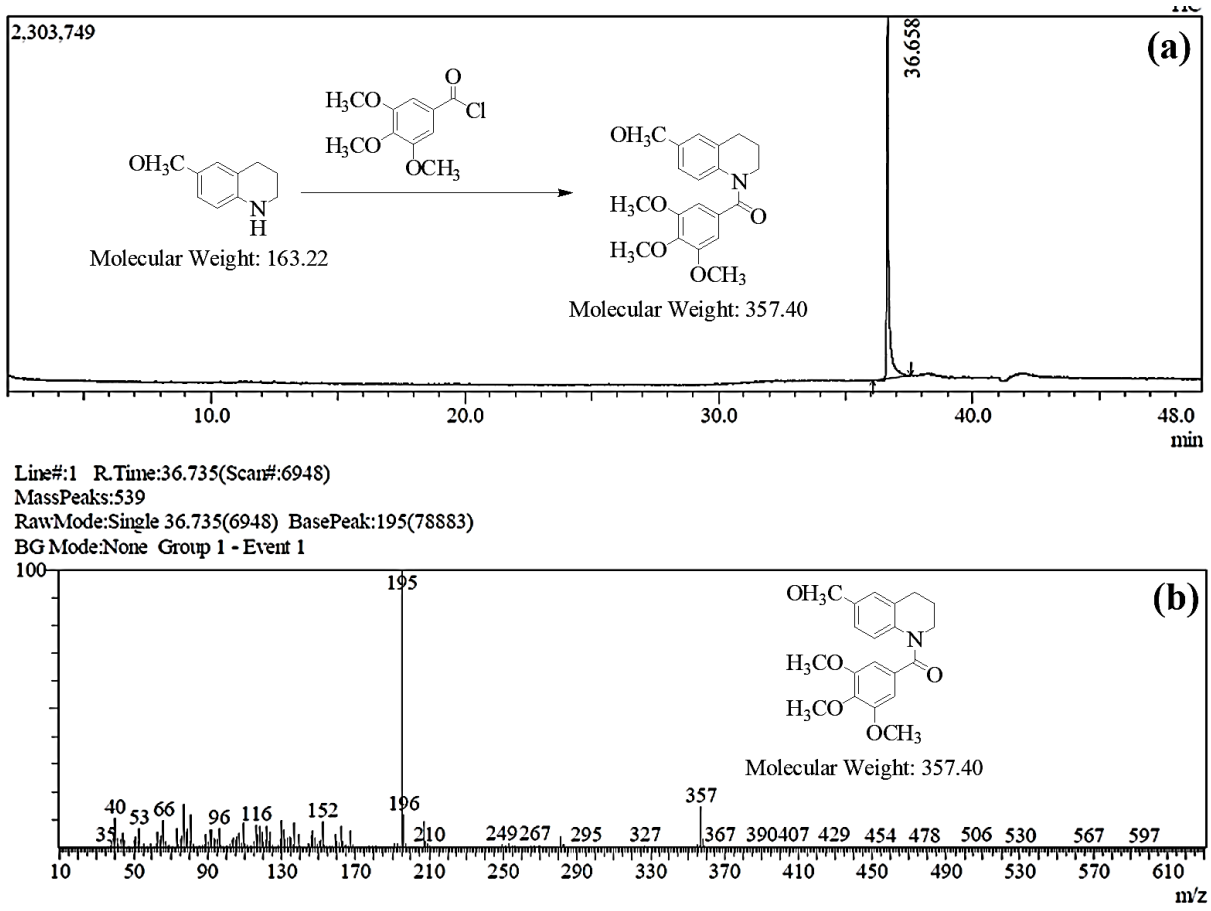

Figure S13. Synthesis of Tubulin polymerization inhibitor from 6-methoxy-1,2,3,4-terahydroquinoline (a) GC and (b) MS spectra.

(END)